Boron Hydride Sheets

International Edition: DOI: 10.1002/anie.201604369
German Edition: DOI: 10.1002/ange.201604369

Two-Dimensional Boron Hydride Sheets: High Stability, Massless Dirac Fermions, and Excellent Mechanical Properties

*Yalong Jiao[+], Fengxian Ma[+], John Bell, Ante Bilic, and Aijun Du**

Abstract: *Two-dimensional (2D) boron sheets have been successfully synthesized in recent experiments, however, some important issues remain, including the dynamical instability, high energy, and the active surface of the sheets. In an attempt to stabilize 2D boron layers, we have used density functional theory and global minimum search with the particle-swarm optimization method to predict four stable 2D boron hydride layers, namely the C2/m, Pbcm, Cmmm, and Pmmn sheets. The vibrational normal mode calculations reveal all these structures are dynamically stable, indicating potential for successful experimental synthesis. The calculated Young's modulus indicates a high mechanical strength for the C2/m and Pbcm phases. Most importantly, the C2/m, Pbcm, and Pmmn structures exhibit Dirac cones with massless Dirac fermions and the Fermi velocities for the Pbcm and Cmmm structures are even higher than that of graphene. The Cmmm phase is reported as the first discovery of Dirac ring material among boron-based 2D structures. The unique electronic structure of the 2D boron hydride sheets makes them ideal for nanoelectronics applications.*

Sitting in between the metals and non-metals in the periodic table, boron is a magic element in the sense that it not only can bond both covalently and ionically,[1] but it is capable of forming a great variety of pure allotropes ranging from 0D clusters,[2] 1D nanotubes,[3] planar 2D sheets,[4] and 3D bulk materials,[5] which exhibit metallic,[6] semimetallic,[7] and semiconducting behavior. It is known that the fabrication of boron layers is quite challenging owing to the multicenter bonding of boron atoms. Nevertheless, very recently 2D borophene,[4a] β_{12}, and χ_3 boron sheets[8] have been successfully synthesized on a Ag (111) surface, which raises further interest in their potential applications, but two significant issues still remain. First, the free-standing borophene is not very stable and its surface is chemically active. The unsaturated boron sheet must be grown on an appropriate substrate that can donate charge and weakly bind with the boron.[9] The boron layers (borophene and β_{12}) obtained also possess very high energy according to a very recent theoretical study.[10] Secondly, the synthesized borophene, β_{12}, and χ_3 sheets are all metallic, and the absence of novel electronic properties limits their potential applications in nanodevices. Therefore, interest has arisen in the search for new boron-based sheets with high stability, low energy, and intriguing electronic states.

Boron atoms are electron-deficient because their three valence electrons can occupy four available orbitals, and therefore exhibit various bonding characters. In an attempt to compensate for the electron-deficiency of boron, hydrogenation is an effective strategy, where a single hydrogen atom can share its electron with the boron atom, and thus the B–H system is isoelectronic with carbon. Such boron hydride (BH) sheets are expected to possess high stability and novel electronic properties such as the Dirac cone feature, which is analogous to graphene and other carbon-based materials. The boron hydride layers also have the potential to form a three-center–two-electron (3c-2e) bond,[11] which is able to stabilize the electron-deficiency of boron networks. Motivated by this, the efforts to search for potentially stable BH sheets with low energy and novel band structures (for example, Dirac cones/ring) are of great interest.

Previous research regarding hydrogenated boron predominantly focused on the hydrogenated cluster form[12] or 2D structures under high pressure.[13] In this work, the particle swarm optimization (PSO) technique has been employed to search for low-energy boron hydride structures with novel electronic properties (specifically, Dirac cone features). In the course of the structure search, a variety of configurations have been produced (some structures are shown in the Supporting Information, Figures S1–S5), but some of them have featureless band structures. Therefore, they are excluded from the further discussion. Four distinctly stable configurations, including the *C*2/*m*, *Pbcm*, *Cmmm*, and *Pmmn* sheets, have been identified as the structures of special interest. The calculations of phonon dispersions and ab initio molecular dynamics (AIMD) simulations confirmed their stability and the investigation of mechanical properties demonstrates their high in-plane stiffness. Most importantly, the *C*2/*m*, *Pbcm*, and *Pmmn* structures exhibit distorted Dirac cones with ultrahigh Fermi velocities. The *Cmmm* phase displays a ring of Dirac nodes[14] in the Brillouin zone, and the present work is the first report of a Dirac ring material in the boron-based 2D material family. This unique Dirac ring band structure is proposed to possess a stronger nonlinear electromagnetic response than a single Dirac cone,[14b] and it is expected to give rise to more intriguing electronic properties and applications.

According to the Aufbau principle,[15] the various boron clusters can be regarded as the fragments from which nanostructures, such as puckered 2D layers, can be constructed. This rule is also applicable in the structures

[*] Y. Jiao,[+] F. Ma,[+] Prof. J. Bell, Prof. A. Du
School of Chemistry, Physics and Mechanical Engineering
Queensland University of Technology
Brisbane, QLD 4001 (Australia)
E-mail: aijun.du@qut.edu.au
Dr. A. Bilic
CSIRO Data61, Docklands 3008 VIC (Australia)
[+] These authors contributed equally to this work.

Supporting information for this article can be found under: http://dx.doi.org/10.1002/anie.201604369.

predicted from the present work. The four typical boron hydride sheets, including the ladder-like cluster[12] extended BH layers (*C*2/*m*), buckled B_7 cluster[15] extended BH sheets (*Pbcm*), hydrogenated graphene-like boron monolayers[16] (*Cmmm*), and 2D hydrogenated borophene (*Pmmn*), are illustrated in Figure 1 a–c and the Supporting Information, Figure S6, respectively. Of the four configurations, the *C*2/*m*

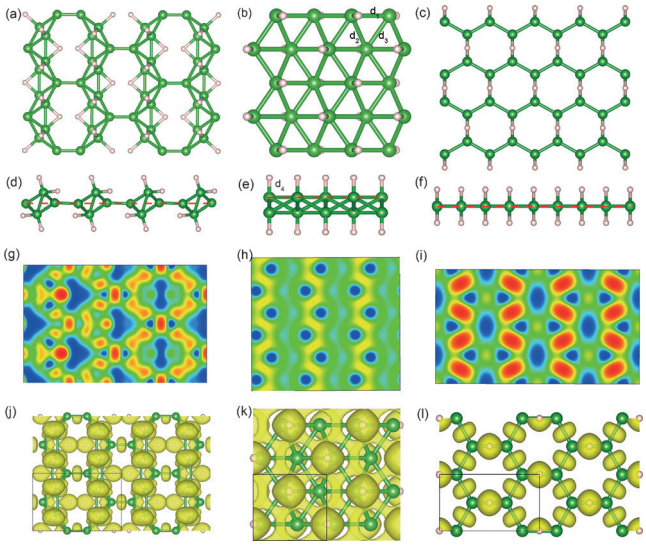

Figure 1. a)–f) Top and side view of *C*2/*m*, *Pbcm*, and *Cmmm* BH structures. g)–i) Slabs cut along (001) direction and ELF for the corresponding structures. j)–l) Side views of the ELF with isovalue of 0.75 for *C*2/*m*, *Pbcm*, and *Cmmm* sheets. The 3c-2e bonds are evident in the *C*2/*m* and *Cmmm* phase.

structure ($B_{12}H_{12}$) has the lowest energy (Table 1). If the *C*2/*m* phase is rotated 30° around the *b* axis (Supporting Information, Figure S7), it becomes evident that it is formed by two ladder-like elongated clusters that look analogous to boron

Table 1: Lattice constants and energy for all predicted BH layers.

Phase	*a* [Å]	*b* [Å]	Energy per atom [eV]	Dirac cone
*C*2/*m*	7.408	4.79	−5.037	yes
Pbcm	3.366	3.024	−5.016	yes
$P\bar{3}$	4.35	4.35	−4.997	no
Cmma	5.215	3.440	−4.957	no
*C*2/*m*	8.282	4.462	−4.946	no
Cmmm	2.988	5.299	−4.901	yes
Pmmn	2.80	1.93	−4.898	yes
*C*2	5.685	3.342	−4.396	no
$P\bar{3}m1$	2.84	2.84	−4.160	no

cluster dihydrides reported previously.[12] However, the *C*2/*m* structure is fully hydrogenated, in contrast to the partially hydrogenated boron clusters. For the *Pbcm* (B_4H_4), it can be viewed as consisting of distorted hexagonal pyramids, which are in fact the buckled B_7 cluster building blocks. This type of cluster has been confirmed as a fragment that is able to form a stable geometry according to the Aufbau principle. The B–B atom distances d_1, d_2, and d_3 are 1.91, 1.88, and 1.83 Å, respectively. The hydrogen atoms alternate on both sides of the boron sheet along the zigzag direction and the B–H bond length is 1.19 Å. For the *Cmmm* structure (B_4H_4), it exhibits a honeycomb graphene-like lattice and the boron sublattice is sandwiched by two layers of hydrogen atoms, which are decorated on both sides of the B–B bonds. The B–B bond length in the honeycomb structure is 1.72 Å, which is longer than the C–C bond in graphene (1.42 Å). The last configuration *Pmmn* is in fact the hydrogenated borophene sheet. However, its energy is 139, 118, and 3 meVatom^{-1} higher than that of the *C*2/*m*, *Pbcm*, and *Cmmm* phase, respectively. The Hirshfeld charge analysis is illustrated in the Supporting Information, Figures S8–S11. By calculating the electron localization function (ELF),[17] the B–B and B–H covalent bonds can be identified in these phases. Additionally, both the σ bonds, formed by the p_x orbitals, and π bonds, formed by the p_y orbitals, can be found in the *C*2/*m* structure (Supporting Information, Figure S12). As the *Pmmn* phase has the highest energy among the four structures, it is omitted from further property discussion.

To examine the dynamical stability of these BH sheets, we calculated their phonon dispersions, as shown in Figure 2. No imaginary modes can be found in the first Brillouin for the *C*2/*m*, *Pbcm*, *Cmmm*, and *Pmmn* phase, indicating their dynamical stability. It should be noted that the synthesized borophene is not dynamically stable, as the existence of an imaginary frequency mode near the Γ point shows.[4a] Nevertheless, this mode can be eliminated by hydrogenation, indicating the effectiveness of this strategy. Additionally, their thermal stability is also confirmed by performing the AIMD simulations shown in the Supporting Information.

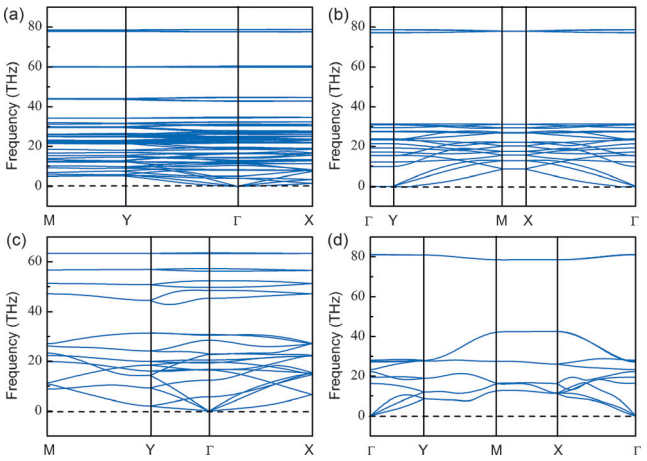

Figure 2. Phonon band structures for a) *C*2/*m*, b) *Pbcm*, c) *Cmmm*, and d) *Pmmn* phases.

The electronic band structure and corresponding total density of states (TDOS) were calculated to examine the electronic properties of the *C*2/*m*, *Pbcm*, and *Cmmm* structures. In Figure 3 a–c, it can be seen that all configurations display a zero-gap semiconducting feature at or in the vicinity of the Fermi level. The meeting points of valence band maximum and conduction band minimum is located at

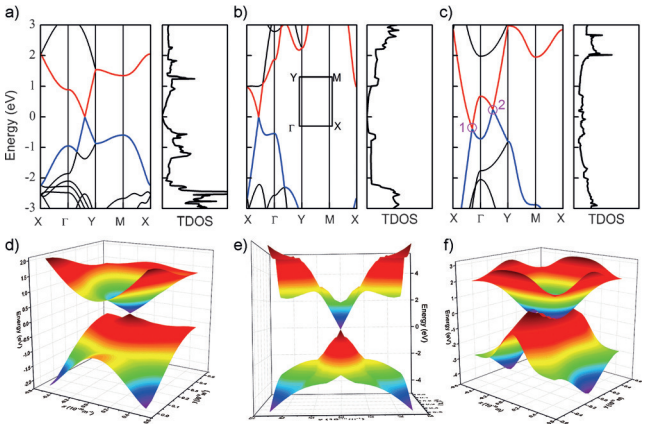

Figure 3. The calculated band structures and total density of states (TDOS) for a) *C*2/*m*, b) *Pbcm*, and c) *Cmmm* structures. d)–f) The 3D band plots for the corresponding phases.

(0, 0.3, 0) along Γ–Y line for *C*2/*m*, and (0.3, 0, 0) along Γ–X line for *Pbcm*. As the TDOS for *C*2/*m* and *Pbcm* are also zero at the Fermi level, such band features can be identified as Dirac points, which is further illustrated by plotting the 3D bands shown in Figure 3 d,e. The *Cmmm* structure exhibits double Dirac cones along the Γ–X and Γ–Y lines (Figure 3 c). The Dirac cone 1 is 0.375 eV below the Fermi level and the cone 2 is 0.233 eV above the Fermi level. By plotting the 3D band (Figure 3 f), it is evident that this structure is not merely a Dirac cone material but, in fact, there is a ring of Dirac nodes in the Brillouin zone. The Dirac ring feature, displaying multiple Dirac cones is a new feature not seen in any other Dirac electron materials such as graphene (with six discrete Dirac points). This ring of Dirac nodes has also been confirmed to be discrete (not continuous) by using a higher precision computation (Supporting Information, Figure S13). Furthermore, the Dirac cone in *C*2/*m*, *Pbcm*, *Cmmm*, and *Pmmn* phase has also been examined by the HSE06 calculations (Supporting Information, Figure S14).

Near the Dirac points exhibiting a linear dispersion, the Fermi velocities v_f were obtained by using the expression $v_f = \partial E/\hbar\partial k$. The calculated v_f for the *C*2/*m* phase is $5.59\times10^5\ m\,s^{-1}$, but the v_f for *Pbcm* ($9.72\times10^5\ m\,s^{-1}$) and cone 1 of *Cmmm* phase ($9.30\times10^5\ m\,s^{-1}$) is even higher than that of graphene ($8.2\times10^5\ m\,s^{-1}$). The Dirac cone-like electronic states demonstrate the excellent electronic transport properties of these 2D BH sheets. To evaluate the robustness of Dirac cones for the *C*2/*m*, *Pbcm*, and *Cmmm* configurations, the tensile/compressive biaxial strains up to 5% are exerted on these sheets. It is found that the strain does not affect the existence of the Dirac cones, only leading to slight change of their Fermi velocities. As the C2/m, *Pbcm*, and *Cmmm* all display linear band dispersions, their effective mass of charge carriers, defined as

$$m^* = \hbar^2\left[\frac{d^2E(k)}{dk^2}\right]^{-1}$$

is zero. Therefore, these phases are expected to have very high carrier mobility.

To explore the origin of the distorted Dirac cone, the orbitally resolved band structures for *Pbcm*, *C*2/*m*, and *Cmmm* are presented. The Dirac cone for *Pbcm* is dominated by the in-plane p_x and p_y orbitals of B atoms (Figure 4 b), which is different from that in the graphene (dominated by

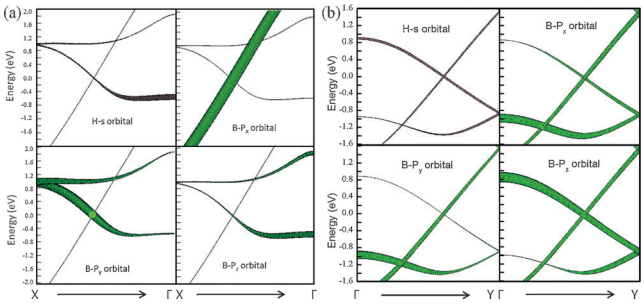

Figure 4. Orbitally resolved band structures for two lowest-energy structures a) *C*2/*m* and b) *Pbcm* phase.

the p_z orbital). Moreover, the Dirac cone for *C*2/*m* phase (Figure 4 a) is dominated by the p_x, p_y, and p_z orbitals of B atoms, while the hybrid of p_x and p_z orbitals make the main contribution to the Dirac cones for the *Cmmm* phase (Supporting Information, Figure S15). The mechanical properties for the *C*2/*m*, *Pbcm*, and *Cmmm* boron layers, namely, the 2D Young's modulus, *Y*, and Poisson's ratio, *ν*, have been evaluated (Supporting Information, Table S1), revealing the high mechanical strength.

The experimental realization of BH sheet is proposed using three possible methods based on the strategies applied to synthesize the boron sheets and hydrogenated graphene.[18] The first approach is a direct synthetic route that is similar to bottom-up approach.[19] Specifically, a pure boron source in hydrogen (H_2) is introduced into an ultra-high vacuum chamber under high frequency plasma, forming the deposited film characterized as boron hydride sheet. The possible substrates include metal or metal boride (for example Ag, Au, or MgB_2). As the functionalization of graphene has been realized by molecular self-assembly,[20] it is also possible to achieve hydrogen functionalization on boron sheets by assembling the boron hydride molecules such as fully hydrogenated ladder-like boron and B7 clusters to form a *C*2/*m* and *Pbcm* phase, respectively. Finally, the atomic exchange with metal borides is also possible. For example, the *Cmmm* structure could be realized through the recently synthesized LiB layer[21] by the displacement reaction: $4\,LiB + 2\,H_2 \rightarrow 4\,Li + B_4H_4$.

In summary, using DFT and performing a particle-swarm structure search, we have identified four stable BH layers with Dirac cone/ring features. The *C*2/*m* sheet possesses the lowest energy among all configurations and the high mechanical strength and ultra-high Fermi velocities make the *Pbcm* sheet an ideal candidate in nanoelectronic device applications. Importantly, the *Cmmm* layer is reported for the first time as the Dirac ring material among boron-based 2D structures. The experimental realization of all of the BH sheets is highly possible owing to their dynamical stability.

This work is an effective effort to design and stabilize the 2D boron sheets, and extend their applications by discovering the novel properties. The synthesis of the predicted structures will significantly enrich the diversity and boost the development of boron-based 2D materials.

Acknowledgements

We acknowledge computer time from HPC facility at QUT and Australian National Facility. A.D. greatly appreciates the ARC QEII Fellowship (DP110101239) and Discovery Project (DP130102420). F.M. acknowledges the support of CSIRO top-up scholarship. A.B. thanks CSIRO for support through the Julius Career Award.

Keywords: boron hydride sheets · density functional theory · Dirac cone · Dirac ring · particle swarm optimization

How to cite: *Angew. Chem. Int. Ed.* **2016**, *55*, 10292–10295
Angew. Chem. **2016**, *128*, 10448–10451

[1] a) A. R. Oganov, J. Chen, C. Gatti, Y. Ma, Y. Ma, C. W. Glass, Z. Liu, T. Yu, O. O. Kurakevych, V. L. Solozhenko, *Nature* **2009**, *457*, 863–867; b) F. Ma, Y. Jiao, G. Gao, Y. Gu, A. Bilic, Z. Chen, A. Du, *Nano Lett.* **2016**, *16*, 3022–3028.

[2] a) T. R. Galeev, C. Romanescu, W.-L. Li, L.-S. Wang, A. I. Boldyrev, *Angew. Chem. Int. Ed.* **2012**, *51*, 2101–2105; *Angew. Chem.* **2012**, *124*, 2143–2147; b) W. Huang, A. P. Sergeeva, H.-J. Zhai, B. B. Averkiev, L.-S. Wang, A. I. Boldyrev, *Nat. Chem.* **2010**, *2*, 202–206; c) L.-M. Yang, E. Ganz, Z. Chen, Z.-X. Wang, P. v. R. Schleyer, *Angew. Chem. Int. Ed.* **2015**, *54*, 9468–9501; *Angew. Chem.* **2015**, *127*, 9602–9637.

[3] V. Bezugly, J. Kunstmann, B. Grundkötter-Stock, T. Frauenheim, T. Niehaus, G. Cuniberti, *ACS Nano* **2011**, *5*, 4997–5005.

[4] a) A. J. Mannix, X.-F. Zhou, B. Kiraly, J. D. Wood, D. Alducin, B. D. Myers, X. Liu, B. L. Fisher, U. Santiago, J. R. Guest, M. J. Yacaman, A. Ponce, A. R. Oganov, M. C. Hersam, N. P. Guisinger, *Science* **2015**, *350*, 1513–1516; b) Z. Zhang, Y. Yang, G. Gao, B. I. Yakobson, *Angew. Chem. Int. Ed.* **2015**, *54*, 13022–13026; *Angew. Chem.* **2015**, *127*, 13214–13218; c) X. Wu, J. Dai, Y. Zhao, Z. Zhuo, J. Yang, X. C. Zeng, *ACS Nano* **2012**, *6*, 7443–7453; d) G. Tai, T. Hu, Y. Zhou, X. Wang, J. Kong, T. Zeng, Y. You, Q. Wang, *Angew. Chem. Int. Ed.* **2015**, *54*, 15473–15477; *Angew. Chem.* **2015**, *127*, 15693–15697; e) R. D. Dewhurst, R. Claessen, H. Braunschweig, *Angew. Chem. Int. Ed.* **2016**, *55*, 4866–4868; *Angew. Chem.* **2016**, *128*, 4948–4950; f) E. S. Penev, A. Kutana, B. I. Yakobson, *Nano Lett.* **2016**, *16*, 2522–2526; g) H. Zhang, Y. Li, J. Hou, K. Tu, Z. Chen, *J. Am. Chem. Soc.* **2016**; h) L. Xu, A. Du, L. Kou, *arXiv preprint arXiv:1602.03620* **2016**; i) Z. Zhang, E. S. Penev, B. I. Yakobson, *Nat. Chem.* **2016**, *8*, 525–527.

[5] B. F. Decker, J. S. Kasper, *Acta Crystallogr.* **1959**, *12*, 503–506.

[6] Z. A. Piazza, H.-S. Hu, W.-L. Li, Y.-F. Zhao, J. Li, L.-S. Wang, *Nat. Commun.* **2014**, *5*, 3113.

[7] X.-F. Zhou, X. Dong, A. R. Oganov, Q. Zhu, Y. Tian, H.-T. Wang, *Phys. Rev. Lett.* **2014**, *112*, 085502.

[8] B. Feng, J. Zhang, Q. Zhong, W. Li, S. Li, H. Li, P. Cheng, S. Meng, L. Chen, K. Wu, *Nat. Chem.* **2016**, *8*, 563–568.

[9] Y. Liu, E. S. Penev, B. I. Yakobson, *Angew. Chem. Int. Ed.* **2013**, *52*, 3156–3159; *Angew. Chem.* **2013**, *125*, 3238–3241.

[10] F. Ma, Y. Jiao, G. Gao, Y. Gu, A. Bilic, Z. Chen, A. Du, *Nano Lett.* **2016**.

[11] W. N. Lipscomb, *Boron hydrides*, Courier Corporation, **2012**.

[12] W.-L. Li, C. Romanescu, T. Jian, L.-S. Wang, *J. Am. Chem. Soc.* **2012**, *134*, 13228–13231.

[13] C.-H. Hu, A. R. Oganov, Q. Zhu, G.-R. Qian, G. Frapper, A. O. Lyakhov, H.-Y. Zhou, *Phys. Rev. Lett.* **2013**, *110*, 165504.

[14] a) B. Zhen, C. W. Hsu, Y. Igarashi, L. Lu, I. Kaminer, A. Pick, S.-L. Chua, J. D. Joannopoulos, M. Soljacic, *Nature* **2015**, *525*, 354–358; b) C. H. Lee, X. Zhang, B. Guan, *Sci. Rep.* **2015**, *5*, 18008.

[15] I. Boustani, *Phys. Rev. B* **1997**, *55*, 16426–16438.

[16] T. A. Abtew, B.-c. Shih, P. Dev, V. H. Crespi, P. Zhang, *Phys. Rev. B* **2011**, *83*, 094108.

[17] a) A. Savin, O. Jepsen, J. Flad, O. K. Andersen, H. Preuss, H. G. von Schnering, *Angew. Chem. Int. Ed. Engl.* **1992**, *31*, 187–188; *Angew. Chem.* **1992**, *104*, 186–188; b) B. Silvi, A. Savin, *Nature* **1994**, *371*, 683–686; c) A. D. Becke, K. E. Edgecombe, *J. Chem. Phys.* **1990**, *92*, 5397–5403.

[18] M. Pumera, C. H. A. Wong, *Chem. Soc. Rev.* **2013**, *42*, 5987–5995.

[19] Y. Wang, X. Xu, J. Lu, M. Lin, Q. Bao, B. Özyilmaz, K. P. Loh, *ACS Nano* **2010**, *4*, 6146–6152.

[20] A. Ciesielski, P. Samori, *Adv. Mater.* **2016**, DOI: 10.1002/adma.201505371.

[21] A. N. Kolmogorov, S. Hajinazar, C. Angyal, V. L. Kuznetsov, A. P. Jephcoat, *Phys. Rev. B* **2015**, *92*, 144110.

Received: May 12, 2016
Revised: June 20, 2016
Published online: July 27, 2016

